

DNA binding, antitumor activities, and hydroxyl radical scavenging properties of novel oxovanadium(IV) complexes with substituted isoniazid

Xiangwen Liao · Jiazheng Lu · Peng Ying ·
Ping Zhao · Yinliang Bai · Wenjie Li ·
Mingpei Liu

Received: 1 June 2013 / Accepted: 1 September 2013 / Published online: 28 September 2013
© SBIC 2013

Abstract Four novel oxovanadium(IV) complexes—[VO(PAHN)(phen)] (**1**; PAHN is 4-pyridinecarboxylic acid, 2-[(2-hydroxy)-1-naphthalenylene] hydrazide, phen is 1,10-phenanthroline), [VO(PAHN)(bpy)] (**2**; bpy is 2,2'-bipyridine), [VO(PAH)(phen)] (**3**; PAH is 4-pyridinecarboxylic acid, 2-[(2-hydroxy)-1-phenyl]methylene hydrazide), and [VO(PAH)(bpy)] (**4**)—have been synthesized and characterized by elemental analysis, UV–vis spectroscopy, electrospray ionization mass spectrometry, IR

spectroscopy, ¹H-NMR spectroscopy, and ¹³C-NMR spectroscopy. Their interactions with calf thymus DNA were investigated. The results suggest that these complexes bind to DNA in an intercalative mode. All four complexes exhibited highly cytotoxic activity against tumor cells (SH-SY5Y, MCF-7, and SK-N-SH), with 50 % inhibitory concentrations of the same order of magnitude as for cisplatin or of lower order of magnitude. Complex **1** exhibited the highest interaction ability and was found to be the most potent antitumor agent among the four complexes. It can cause G₂/M phase arrest of the cell cycle, induces significant apoptosis in SK-N-SH cells, and displays typical morphological apoptotic characteristics. In addition, their hydroxyl radical scavenging properties have been tested, and complex **1** was the best inhibitor.

Electronic supplementary material The online version of this article (doi:10.1007/s00775-013-1046-9) contains supplementary material, which is available to authorized users.

X. Liao · J. Lu (✉) · P. Ying
School of Pharmacy,
Guangdong Pharmaceutical University,
Guangzhou 510006,
Guangdong, People's Republic of China
e-mail: lujia6812@163.com

P. Zhao (✉)
School of Medicine Chemistry and Chemical Engineering,
Guangdong Pharmaceutical University,
Guangzhou 510006, Guangdong, People's Republic of China
e-mail: zhaoping666@163.com

Y. Bai · M. Liu
Department of Pharmacy, Lanzhou University Second Hospital,
No. 82, Cuiyingmen, Lanzhou 730030, Gansu, People's
Republic of China

W. Li
Department of Clinical Pharmacology,
School of Pharmaceutical Sciences,
Zhengzhou University, Zhengzhou 450001,
Henan, People's Republic of China

Keywords Oxovanadium complexes · DNA binding ·
Cleavage · Antitumor · Scavenging hydroxyl radical

Abbreviations

CT-DNA	Calf thymus DNA
DMF	<i>N,N</i> -Dimethylformamide
DMSO	Dimethyl sulfoxide
ESI-MS	Electrospray ionization mass spectrometry
H ₄ EDTA	<i>N,N'</i> -1,2-Ethanediybis[<i>N</i> -(carboxymethyl)]glycine
IC ₅₀	50 % inhibitory concentration
MTT	3-(4,5-Dimethylthiazoyl-2-yl)-2,5-diphenyltetrazolium bromide
PAH	4-Pyridinecarboxylic acid, 2-[(2-hydroxy)-1-phenyl]methylene hydrazide
PAHN	4-Pyridinecarboxylic acid, 2-[(2-hydroxy)-1-naphthalenylene] hydrazide
PI	Propidium iodide
Tris	Tris(hydroxymethyl)aminomethane

Introduction

In the last few decades, metal complexes has received much attention owing to their huge potential as antitumor agents, such as ruthenium complexes, cobalt(II) complexes, copper complexes, gold complexes, and platinum complexes [1–5]. Vanadium, as a trace bioelement, exhibits a variety of biological activities, such as antitumor, antimicrobial, and insulin-enhancing effects, and exhibits potent anti-HIV effects toward infected immortalized T cells [6–12]. Many oxovanadium(IV) complexes with various coordination modes have been prepared, viz., VO(O₄), VO(S₂N₂), VO(S₄), VO(N₃O), and VO(N₂O₂), and the relationship between their structures and insulin-mimetic activities has been examined by evaluating both in vivo and in vitro results [13–16]. Bis(ethylmaltolato)oxovanadium(IV) has completed a phase I clinical trial in humans for the treatment of type 1 and type 2 diabetes mellitus [17–19]. More recently, vanadium has attracted the attention of researchers because of its wide distribution and broad biological activity [20–22], particularly after the discovery of its involvement in DNA-repair systems [23, 24]. Vanadium-containing compounds have also shown great potential as inhibitors of chemically induced tumors in test animals and cell cultures in vitro, being efficient, for example, in the treatment of leukemia, breast adenocarcinoma, and Ehrlich tumors in marines, and lung, breast, ovarian, testicular, renal, gastrointestinal, and nasopharyngeal carcinomas in humans [23–26]. The role of vanadium in the prevention of DNA–protein cross-links, DNA chain breaks, and chromosomal aberrations has been documented. Research on the cancer therapeutic role of vanadium has progressed to the preclinical stage in vivo [27, 28].

Keeping in view the significant bioactive nature of a Schiff base as well as the biological functioning of vanadium, it was thought valuable to merge the chemistry of Schiff bases with that of vanadium to form a novel class of vanadium-metal-based Schiff bases that could serve as potential antitumor agents against resistant cancer cells [16, 28]. It is known that complexes causing photocleavage of DNA and exhibiting photocytotoxic properties in visible light are of importance as chemotherapeutic agents [20–26]. Great efforts have, therefore, been made to synthesize oxovanadium(IV) complexes of high biological activity and low toxicity which are readily absorbed [24, 25, 27]. Previously, we reported that four oxidovanadium(IV) complexes interact with DNA through an intercalative mode and can efficiently cleave plasmid pBR 322 DNA. More interestingly, these oxidovanadium(IV) complexes exhibit highly cytotoxic activities against myeloma cell (Ag8.653) and glioma cell (U251) lines. Especially, among complexes with thiosemicarbazones, [VO(hntdtsc)(phen)]

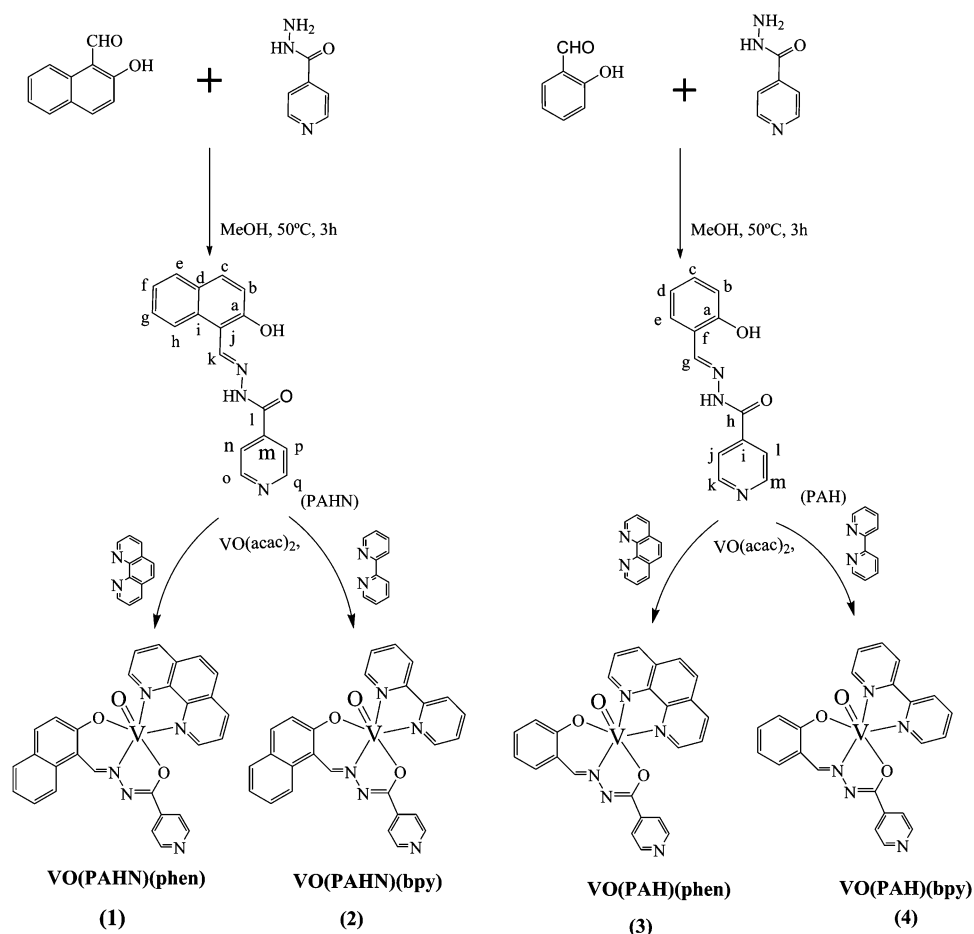
(hntdtsc is 2-hydroxy-1-naphthaldehyde thiosemicarbazone, phen is 1,10-phenanthroline) was found to be a promising compound with potential in the treatment of cancer cells, and its 50 % inhibitory concentration (IC₅₀) is very close to that of cisplatin [29]. Our previous results also indicated that with increasing the appending aromatic moiety, the activity of vanadium complexes would much better [29–31].

To further our studies in this model system, four new oxovanadium(IV) complexes—[VO(PAHN)(phen)] (1; PAHN is 4-pyridinecarboxylic acid, 2-[(2-hydroxy)-1-naphthalenylene] hydrazide), [VO(PAHN)(bpy)] (2; bpy is 2,2'-bipyridine), [VO(PAH)(phen)] (3; PAH is 4-pyridinecarboxylic acid, 2-[(2-hydroxy)-1-phenyl]methylene hydrazide), and [VO(PAH)(bpy)] (4)—have been synthesized (Scheme 1) and characterized by elemental analysis, UV–vis spectroscopy, electrospray ionization mass spectrometry (ESI-MS), IR spectroscopy, ¹H-NMR spectroscopy, and ¹³C-NMR spectroscopy. The interaction of these complexes with calf-thymus DNA (CT-DNA) was investigated using UV–vis absorption spectroscopy, fluorescence spectroscopy, viscosity measurements, and thermal denaturation studies. Their cytotoxicity toward a human breast cancer cell line (MCF-7) and human neuroblastoma cells (SH-SY5Y and SK-N-SH) was investigated by 3-(4,5-dimethylthiazoyl-2-yl)-2,5-diphenyltetrazolium bromide (MTT) assay. In addition, their hydroxyl radical scavenging properties were investigated.

Materials and methods

Materials

VO(acac)₂ (acac is acetylacetonate), 1,10-phenanthroline, 2,2'-bipyridine, and isonicotinic acid hydrazide were purchased from Shanghai Jingchun. CT-DNA was obtained from Sigma. SH-SY5Y, SK-N-SH (derived from human neuroblastoma cell lines), and MCF-7 (breast cancer cell line isolated from human mammary glands) cell lines were purchased from the Cell Bank of Type Culture Collection of the Chinese Academy of Sciences (Shanghai, China). Hoechst 33342 staining solution was purchased from Beyotime Institute of Biotechnology (China). MTT and rhodamine 123 were purchased from Sigma (USA). Other materials were obtained from commercial sources and used as received (analytical reagents). Tris(hydroxymethyl)aminomethane (Tris)–HCl buffer A (5 mM Tris–HCl and 50 mM NaCl, pH 7.2) was used for absorption titration, luminescence titration, and viscosity experiments. Tris–HCl buffer B (50 mM Tris–HCl and 18 mM NaCl, pH 7.2) was used for DNA-cleavage experiments. Buffer C (1.5 mM NaHPO₄, 0.5 mM NaH₂PO₄, and 0.25 mM

Scheme 1 The synthetic routes for the ligands and complexes

$\text{Na}_2\text{H}_2\text{EDTA}$ pH 7.0; H_4EDTA is *N,N'*-ethane-1, 2-diyl-bis[*N*-(carboxymethyl)glycine]) was used for thermal denaturation. All buffers were prepared using double-distilled water. A solution of CT-DNA in the buffer gave a ratio of the UV absorbance at 260 and 280 nm of approximately 1.8–1.9, indicating that the DNA was sufficiently free of protein [32–34]. The DNA concentration per nucleotide was determined by absorption spectroscopy using the molar absorption coefficient ($6,600 \text{ M}^{-1} \text{ cm}^{-1}$) at 260 nm [35–37]. DNA stock solutions were stored at 4 °C and used after no more than 3 days. Solutions of compounds were freshly prepared 1 h prior to biochemical evaluation.

Physical measurements

Microanalysis (C, H, S, and N) was conducted with a PerkinElmer 240Q elemental analyzer. Electrospray ionization mass spectra were recorded with an LCQ system (Finnigan MAT, USA) using methanol as the mobile phase. IR spectra were recorded with a PerkinElmer Lambda 35 instrument using KBr pellets. $^1\text{H-NMR}$ and $^{13}\text{C-NMR}$ spectra were recorded with a Varian 500 spectrometer. All

chemical shifts are given relative to tetramethylsilane. UV–vis absorption spectra were recorded with a Shimadzu UV-3101 PC spectrophotometer at room temperature. Emission spectra were recorded with a Perkin-Elmer Lambda 55 spectrofluorophotometer. Molar conductivities in 1mM *N,N*-dimethylformamide (DMF) solution at room temperature were measured using a DDS-307 digital direct reading conductivity meter.

Cell viability assay was performed with a microplate reader (model 680, Bio-Rad, USA). Cell cycle analysis, annexin V–fluorescein isothiocyanate/propidium iodide (PI) assay of apoptotic cells and detection of mitochondrial membrane potential were performed with a FACScan flow cytometer (BD, USA). Fluorescence microscopy of apoptosis assays was performed with an OX31 fluorescence microscope (Olympus, Japan).

Data were expressed as the mean \pm the standard deviation from three independent experiments. Statistical analysis was performed using SPSS 13.0 for Windows. Comparisons between two groups were performed by an unpaired *t* test. Multiple comparisons between more than two groups were performed by one-way analysis of variance. Significance was accepted at a *P* value lower than 0.05.

Synthesis of PAHN

PAHN was synthesized with a method similar that described earlier (see Scheme 1) [29–32]. To a stirring solution of 2-hydroxy-1-naphthaldehyde (0.8609 g, 5 mmol) in 10 mL of absolute alcohol was added dropwise isonicotinic acid hydrazide (0.685 g, 5 mmol), which was dissolved in 10 mL of absolute alcohol. Then the mixture was stirred continuously at 50 °C for 3 h, resulting in a yellow gossypine precipitate, which was used without further purification. Yield: 0.7569 g, 52 %. Anal. Calcd for $C_{17}H_{13}N_3O_2$ (%): C, 70.09; H, 4.50; N, 14.42; O, 10.98. Found (%): C, 70.01; H, 4.49; N, 14.31; O, 10.87. ESI-MS (CH_3OH , m/z): 292.1 ($[M + H]^+$). IR (KBr) (ν_{max} , cm^{-1}): 3,450 (s) (O–H), 3,169 (s) (N–H), 1,610 (s) (C=N), 1,571 (m) (C=O). 1H -NMR (500 MHz, dimethyl- d_6 sulfoxide, DMSO- d_6 , ppm): 12.52 (s, 1H, NHCO), 12.40 (s, 1H, OH), 9.48 (s, 1H, CH=N), 8.80 (dd, 2H, ArH, $J = 8.0$ Hz), 8.31 (d, 1H, ArH, $J = 7.8$ Hz), 7.97 (d, 1H, ArH, $J = 8.2$ Hz), 7.88 (br, 3H, ArH, $J = 8.7$ Hz), 7.62 (t, 1H, ArH, $J = 8.3$ Hz), 7.41 (t, 1H, ArH, $J = 8.1$ Hz), 7.26 (d, 1H, ArH, $J = 7.9$ Hz). ^{13}C -NMR (500 MHz, DMSO- d_6 , ppm): 108.5 C (j), 118.8 C (h), 120.9 C (b), 121.4 C (n, p), 123.6 C (f), 127.8 C (g), 127.9 C (e), 128.9 C (d), 131.6 C (c), 133.2 C (i), 139.8 C (m), 147.9 C (k), 150.4 C (o,q), 158.1 C (l), 161.0 C (a). UV–vis λ_{max} , nm (ϵ , $M^{-1} cm^{-1}$) in DMSO: 340 (25,320).

Synthesis of PAH

PAH was prepared using a procedure similar to that used for PAHN, with salicylaldehyde (0.6106 g, 5 mmol) in place of 2-hydroxy-1-naphthaldehyde. This gave a white precipitate, which was used without further purification. Yield: 0.7351 g, 61 %. Anal. Calcd for $C_{13}H_{11}N_3O_2$ (%): C, 64.72; H, 4.60; N, 17.42; O, 13.26. Found (%): C, 64.13; H, 4.51; N, 17.33; O, 13.03. ESI-MS (CH_3OH , m/z): 242.0 ($[M + H]^+$). IR (KBr) (ν_{max} , cm^{-1}): 3,443 (s) (O–H), 3,208 (s) (N–H), 1,603 (s) (C=N), 1,538 (s) (C=O). 1H -NMR (500 MHz, DMSO- d_6 , ppm): 12.29 (s, 1H, NHCO), 11.07 (s, 1H, OH), 8.80 (dd, 2H, ArH, $J = 8.1$ Hz), 8.68 (s, 1H, CH=N), 7.78 (d, 1H, ArH, $J = 8.3$ Hz), 7.61 (m, 1H, ArH, $J = 7.9$ Hz), 7.32 (dd, 2H, ArH, $J = 8.4$ Hz), 6.92 (m, 2H, ArH, $J = 8.0$ Hz). ^{13}C -NMR (500 MHz, DMSO- d_6 , ppm): 116.4 C (b), 118.7 C (f), 119.4 C (d), 121.5 C (j, l), 129.2 C (e), 131.7 C (c), 139.9 C (i), 148.9 C (g), 150.4 C (k,m), 157.5 C (a), 161.3 C (h). UV–vis λ_{max} , nm (ϵ , $M^{-1} cm^{-1}$) in DMSO: 341 (25,320).

Synthesis of complex 1

Complex 1 was obtained as reddish-brown powder by refluxing a mixture of PAHN (0.145 g, 0.5 mmol) and 1,10-

phenanthroline (0.0901 g, 0.5 mmol) in absolute methanol (100 mL) at 80 °C under argon for 2 h. Then the solid powder was isolated from the hot solution and washed with absolute methanol and diethyl ether, respectively, and dried in vacuo. Yield: 0.1747 g, 65.2 %. Anal. Calcd for $C_{29}H_{19}N_5O_3V$ (%): C, 64.93; H, 3.57; N, 13.06; O, 8.95. Found (%): C, 64.75; H, 3.51; N, 13.03; O, 8.90. ESI-MS (CH_3OH , m/z): 537.0 ($[M + H]^+$). IR (KBr) (ν_{max} , cm^{-1}): 1,589 (s) (C=N), 1,568 (m) (C=O), 955 (s) (V–O), 702 (s) (V–N). 1H -NMR (500 MHz, DMSO- d_6 , ppm): 9.15 (s, 1H, CH=N), 8.62 (br, 3H, ArH, $J = 8.5$ Hz), 8.50 (t, 6H, ArH, $J = 8.2$ Hz), 8.09 (s, 2H, ArH), 7.87 (br, 3H, ArH, $J = 7.9$ Hz), 7.61 (m, 3H, ArH, $J = 8.2$ Hz), 6.82 (s, 1H, ArH). UV–vis λ_{max} , nm (ϵ , $M^{-1} cm^{-1}$) in DMSO: 264 (43,870), 341 (14,246), 385 (6,535). Magnetic moment μ_{eff} : 1.68 μ_B . Ω_M ($S m^2 mol^{-1}$): 30.9.

Synthesis of complex 2

Complex 2 was synthesized by a procedure similar to that used for complex 1, with 2,2'-bipyridine (0.0781 g, 0.5 mmol) in place of 1,10-phenanthroline. Yield: 0.1634 g, 63.8 %. Anal. Calcd for $C_{27}H_{19}N_5O_3V$ (%): C, 63.29; H, 3.74; N, 13.67; O, 9.37. Found (%): C, 63.01; H, 3.51; N, 13.03; O, 9.35. ESI-MS (CH_3OH , m/z): 513.1 ($[M + H]^+$). IR (KBr) (ν_{max} , cm^{-1}): 1,618 (s) (C=N), 1,584 (s) (C=O), 954 (s) (V–O), 722 (s) (V–N). 1H -NMR (500 MHz, DMSO- d_6 , ppm): 9.46 (s, 1H, CH=N), 8.63 (d, 2H, ArH, $J = 8.0$ Hz), 8.38 (m, 2H, ArH, $J = 8.3$ Hz), 7.93 (br, 6H, ArH, $J = 8.7$ Hz), 7.54 (br m, 6H, ArH, $J = 8.4$ Hz), 7.25 (m, 2H, ArH, $J = 8.0$ Hz). UV–vis λ_{max} , nm (ϵ , $M^{-1} cm^{-1}$) in DMSO: 264 (43,650), 341 (14,250), 376 (6,532). Magnetic moment μ_{eff} : 1.72 μ_B . Ω_M ($S m^2 mol^{-1}$): 28.5.

Synthesis of complex 3

Complex 3 was synthesized by a procedure similar to that used for complex 1, with PAH (0.120 g, 0.5 mmol) in absolute methanol (30 mL) in place of PAHN in absolute methanol (100 mL). Yield: 0.1385 g, 57 %. Anal. Calcd for $C_{25}H_{17}N_5O_3V$ (%): C, 61.74; H, 3.52; N, 14.40; O, 9.87. Found (%): C, 61.13; H, 3.51; N, 14.23; O, 9.83. ESI-MS (CH_3OH , m/z): 487.0 ($[M + H]^+$). IR (KBr) (ν_{max} , cm^{-1}): 1,610 (s) (C=N), 1,589 (s) (C=O), 955 (s) (V–O), 727 (s) (V–N). 1H -NMR (500 MHz, DMSO- d_6 , ppm): 9.87 (s, 1H, CH=N), 8.75 (br, 1H, ArH, $J = 8.7$ Hz), 8.42 (m, 3H, ArH, $J = 7.8$ Hz), 7.95 (br, 3H, ArH, $J = 8.4$ Hz), 7.86 (d, 2H, ArH, $J = 8.2$ Hz), 7.57 (br m, 3H, ArH, $J = 8.0$ Hz), 7.31 (m, 2H, ArH, $J = 8.0$ Hz), 7.08 (m, 2H, ArH, $J = 8.2$ Hz). UV–vis λ_{max} , nm (ϵ , $M^{-1} cm^{-1}$) in DMSO: 265 (41,760), 345 (15,245), 378 (6,475). Magnetic moment μ_{eff} : 1.69 μ_B . Ω_M ($S m^2 mol^{-1}$): 40.1.

Synthesis of complex 4

Complex **4** was synthesized by a procedure similar to that used for complex **3**, with 2,2'-bipyridine (0.0781 g, 0.5 mmol) in place of 1,10-phenanthroline. Yield: 0.1053 g, 45.6 %. Anal. Calcd for C₂₃H₁₇N₅O₃V (%): C, 59.75; H, 3.71; N, 15.15; O, 10.38. Found (%): C, 59.73; H, 3.41; N, 15.13; O, 10.23. ESI-MS (CH₃OH, *m/z*): 463.0 ([M + H]⁺). IR (KBr) (ν_{\max} , cm⁻¹): 1,610 (s) (C=N), 1,589 (s) (C=O), 955 (s) (V–O), 699 (s) (V–N). ¹H-NMR (500 MHz, DMSO-*d*₆, ppm): 9.25 (s, 1H, CH=N), 8.69 (s, 3H, ArH), 8.40 (br, 4H, ArH, *J* = 8.4 Hz), 7.96 (m, 3H, ArH, *J* = 8.2 Hz), 7.46 (s, 2H, ArH, *J* = 8.0 Hz), 6.94 (br, 2H, ArH, *J* = 7.8 Hz), 6.79 (m, 2H, ArH, *J* = 8.2 Hz). UV–vis λ_{\max} , nm (ϵ , M⁻¹ cm⁻¹) in DMSO: 265 (41,770), 345 (15,258), 380 (6,455). Magnetic moment μ_{eff} : 1.73 μ_{B} . Ω_{M} (S m² mol⁻¹): 37.9.

DNA binding

Absorption titration experiments were performed with fixed concentrations of the complexes (20 μM), while gradually increasing the concentration of CT-DNA. Vanadium–DNA solutions were incubated for 5 min before the absorption spectra were recorded. To compare the binding strength of the complexes, their intrinsic binding constants (K_{b}) were determined by monitoring the changes in absorbance in the ligand transfer band with increasing concentration of CT-DNA. K_{b} was then calculated using the following equation [35–40]:

$$\frac{[\text{DNA}]}{\epsilon_{\text{a}} - \epsilon_{\text{f}}} = \frac{[\text{DNA}]}{\epsilon_{\text{b}} - \epsilon_{\text{f}}} + \frac{1}{K_{\text{b}}(\epsilon_{\text{b}} - \epsilon_{\text{f}})} \quad (1)$$

where [DNA] is the concentration of DNA in base pairs, ϵ_{a} is the extinction coefficient observed for $A_{\text{obs}}/[V]$, ϵ_{b} is the extinction coefficient of the complex when fully bound to DNA, and ϵ_{f} is the extinction coefficient of the complex free in solution.

Viscosity measurements were performed with a Ubbelohde viscometer maintained at a constant temperature of (28 \pm 0.1) $^{\circ}\text{C}$ in a thermostatic bath. A digital stopwatch was used to measure the flow time, and each sample was measured five times to obtain the average flow time. Data are presented as $(\eta/\eta_0)^{1/3}$ versus the binding ratio, where η is the viscosity of DNA in the presence of the complexes and η_0 is the viscosity of DNA alone [29, 30].

Thermal denaturation studies were performed with a Shimadzu UV-3101 PC spectrophotometer equipped with a Peltier temperature-controlling programmer (± 0.1 $^{\circ}\text{C}$). The melting curves were obtained by measuring the absorbance at 260 nm for solutions of CT-DNA (80 μM) in the absence and presence of the oxovanadium complex

(20 μM) as a function of temperature. The temperature was scanned from 50 to 90 $^{\circ}\text{C}$ at a speed of 5 $^{\circ}\text{C min}^{-1}$.

Cytotoxicity assay

The cytotoxicity of the oxovanadium(IV) complexes was tested in SH-SY5Y, MCF-7, and SK-N-SH human cancer cell lines using MTT assay. The compounds were first dissolved in DMSO (less than 0.1 %) and were then diluted with RPMI 1640 to the required concentrations prior to use. The control was prepared by addition of culture medium (100 μL). Wells containing culture medium without cells were used as blanks. SH-SY5Y, MCF-7, and SK-N-SH cells at a density 2×10^4 cells per well were precultured in 96-well microtiter plates for 48 h at 37 $^{\circ}\text{C}$, 5 % CO₂. On completion of the incubation, stock MTT dye solution was added to each well. After 4 h incubation, a solution containing DMF (50 %) and sodium dodecyl sulfate (20 %) was added to solubilize the MTT formazan. The cell viability was determined by measuring the absorbance of each well at 490 nm using a Multiskan SSCENT microplate reader. IC₅₀ values were determined by plotting the percentage viability versus concentration on a logarithmic graph and reading off the concentration at which 50 % of cells remain viable relative to the control cells (0.5 % DMSO) [28, 29, 41–43]. Cultures were duplicated for each experimental point in at least three independent experiments. The same batches of culture medium, sera, and reagents were used throughout the study.

Cell cycle analysis

The cell cycle of control and treated cancer cells was analyzed. With use of standard methods, the DNA of cells was stained with PI, and the proportions of nonapoptotic cells in different phases of the cell cycle were recorded [28, 44–46]. The cancer cells were treated with the complexes, harvested by centrifugation at 1,000g for 5 min, and then washed with ice-cold phosphate buffer solution. The cells collected were fixed overnight with cold 70 % ethanol, and were then stained with PI solution consisting of 50 $\mu\text{g mL}^{-1}$ PI and 10 $\mu\text{g mL}^{-1}$ RNase. After 10 min incubation at room temperature in the dark, fluorescence-activated cells were sorted in a FACScan flow cytometer using the Cell Quest 3.0.1 software program. The percentage of cells in each phase of the cell cycle was determined at least in triplicate and was expressed as the mean \pm the standard deviation.

Fluorescence microscopy of apoptosis assays

The apoptosis assay method was modified from that in a previous report [28, 47–50]. Briefly, after exposure to the

oxovanadium complexes for 48 h, the cancer cells were washed twice with phosphate buffer solution, and were then stained with $10 \mu\text{g mL}^{-1}$ Hoechst 33342 staining solution at 37°C for 30 min according to the manufacturer's instructions. Finally, the cells were observed under a fluorescence microscope.

Scavenging of the hydroxyl radical

The hydroxyl radical in aqueous media was prepared by the Fenton reaction [51–54]. Solutions of the test complexes were prepared with DMF. The 4 mL of the assay mixture contained the following reagents: the test compounds (2.0 – $5.0 \mu\text{M}$), safranin ($28.5 \mu\text{M}$), EDTA-Fe(II) ($100 \mu\text{M}$), H_2O_2 ($44.0 \mu\text{M}$), and a phosphate buffer (67 mM , $\text{pH } 7.4$). The absorbance of the assay mixture was measured at 520 nm after incubation at 37°C for 15 min in a water bath. All the tests were performed in triplicate and the results were expressed as the mean. The scavenging ratio was calculated on the basis of $(A_i - A_0)/(A_c - A_0) \times 100 \%$, where A_i is the absorbance in the presence of the test complex, A_0 is the absorbance in the absence of the test complex, and A_c is the absorbance in the absence of the test complex and EDTA-Fe(II).

Results and discussion

Synthesis and characterization

The ligands PAHN and PAH were easily synthesized in high yield by refluxing a mixture of isonicotinic acid hydrazide with 2-hydroxy-1-naphthaldehyde and salicylaldehyde, respectively, in absolute methanol. Complexes **1–4** were prepared by refluxing $\text{VO}(\text{acac})_2$ with 1,10-phenanthroline and 2,2'-bipyridine in absolute methanol. The synthesis routes of the complexes and ligands are shown in Scheme 1. All complexes and ligands were characterized by elemental analysis, ESI-MS, IR, UV-vis spectroscopy, $^1\text{H-NMR}$ spectroscopy, and $^{13}\text{C-NMR}$ spectroscopy.

The IR spectra of the free forms of the ligands were compared with the spectra of the vanadium complexes (Table S1). A signal for V–N stretch was observed for complexes **1–4** at 702 , 722 , 727 , and 699 cm^{-1} , respectively, and $\nu(\text{V-O})$ stretching for the complexes occurred at approximately 955 cm^{-1} as reported for other oxovanadium derivatives [14, 17, 23–25].

The $^1\text{H-NMR}$ and $^{13}\text{C-NMR}$ spectral data of the free forms of the ligands recorded in $\text{DMSO-}d_6$ and the possible assignments were reported in “Materials and methods.” All the protons due to heteroaromatic groups and the carbons were found in the expected regions [24, 28].

The electronic spectra of the oxovanadium(IV) complexes and the ligands were reported in “Materials and methods.” As for the ESI-MS spectra, the Schiff base ligands, PAHN and PAH, showed peaks at m/z 292.0 ($[\text{M} + \text{H}]^+$) and 242.0 ($[\text{M} + \text{H}]^+$), respectively. The oxovanadium(IV) complexes were found at m/z 536.0 ($[\text{M} + \text{H}]^+$) (**1**), 512.0 ($[\text{M} + \text{H}]^+$) (**2**), 486.0 ($[\text{M} + \text{H}]^+$) (**3**), and 462.0 ($[\text{M} + \text{H}]^+$) (**4**), respectively.

The molar conductivities of complexes **1–4** were recorded in DMF and fall in the range 28 – $37 \text{ S m}^2 \text{ mol}^{-1}$ (Table S2), which is low for them to be regarded as non-electrolytic [28, 29, 32]. The magnetic moments (1.68 – $1.75 \mu_{\text{B}}$) were obtained at room temperature (Table S2). These values are close to the reported values for a square-pyramidal geometry [28–34]. The elemental analysis, UV-vis spectroscopy, ESI-MS, IR spectroscopy, $^1\text{H-NMR}$ spectroscopy, and $^{13}\text{C-NMR}$ spectroscopy results for all the compounds are in agreement with the proposed structures shown in Scheme 1.

In addition, no change was observed in the UV-vis absorption spectra of all the compounds after the solutions had been diluted with water, indicating that the compounds are stable in water.

DNA-binding studies

Absorption titrations and fluorescence spectroscopy studies

Absorption titration in the UV-vis range was used to investigate the interaction of the four oxovanadium(IV) complexes with CT-DNA. The interaction of the complexes with the base pairs of DNA is accompanied by hypochromism and bathochromism [29, 35], which is mainly attribute to the stacking interaction between the planar aromatic chromophore of the complexes and the base pairs of DNA. For metal interaction, DNA binding is associated with hypochromism and a redshift in the metal-to-ligand charge transfer and ligand bands [35–37].

In the electronic spectra, appreciable hypochromism and bathochromism can be observed for the four complexes with increasing amounts of DNA. The specific hypochromism and bathochromism of the four complexes were 24 % and 2 nm (**1**), 12 % and 2 nm (**2**), 10.5 % and 2 nm (**3**), and 8.7 % and 1 nm (**4**), respectively (Fig. S1). According to previously reported results [34–39], the UV-vis spectral characteristics suggest that complexes **1–4** interact with DNA most likely through a mode that involves a stacking interaction between the aromatic chromophore and the base pairs of DNA. The intrinsic binding constant, K_b , decreases in the order **1** > **2** > **3** > **4**. The differences in their binding strength may be due to the presence of an appending aromatic moiety in PAHN, and this explains the larger binding affinities of the

corresponding complexes in comparison with those of complexes incorporating PAH [33, 38, 44]. The results also imply that the interactions of these complexes with DNA may be mainly through the PAHN and PAH plane and base pairs, and show a classic intercalative mode. Furthermore, the electronic effect of 1,10-phenanthroline or 2,2'-bipyridine is one of the factors determining the binding affinities. Probably, the absence of substituents on the phenol ring may improve the intercalation ability of the vanadyl complex. The DNA-binding affinity (K_b value) was slightly smaller than for VO(SAA)(phen), VO(MOSAA)(phen), and other previously reported complexes [29–32]. The different results might be due to the different electrochemical performances and the influence of different ligand systems [29, 33, 38, 44].

To compare quantitatively the DNA-binding strengths of these complexes, the intrinsic binding constant K_b was calculated from the changes in absorbance in the ligand charge transfer bands with increasing amounts of CT-DNA. The values of K_b were calculated using Eq. 1 to be $(2.70 \pm 0.10) \times 10^4$, $(2.10 \pm 0.10) \times 10^4$, $(1.60 \pm 0.10) \times 10^3$, and $(1.18 \pm 0.10) \times 10^4 \text{ M}^{-1}$ for complexes **1**, **2**, **3**, and **4**, respectively. These K_b values are in the range observed for previously reported complexes [23].

Fluorescence spectroscopy was used to study interactions of the complexes with CT-DNA in Tris buffer A at room temperature [29–31]. With increasing concentrations of CT-DNA, the emission intensities of complexes **1–4** increase by about 1.40 ± 0.01 , 1.38 ± 0.01 , 1.25 ± 0.01 , and 1.13 ± 0.01 times at about 700 nm, respectively, in comparison with those of the complexes alone (Fig. S2). On the other hand, the enhancement of emission intensity is indicative of binding of the complexes to the hydrophobic pocket of DNA, since the hydrophobic environment inside the DNA helix reduces the accessibility of water molecules to the complex and the mobility of the complex is restricted at the binding site, leading to a decrease of the vibrational modes of relaxation, thus lengthening the luminescence lifetimes and increasing emission intensity [33, 38, 44–46]. This observation is consistent with the results of the UV–vis experiments.

Viscosity measurements and thermal denaturation studies

Hydrodynamics (viscosity) experiments are useful to detect intercalation between small molecules and DNA in the absence of crystallographic structural data. When a complex binds to DNA by intercalation, the base pairs are separated to accommodate the binding ligand, resulting in lengthening of the DNA helix, and so increasing the viscosity of the DNA solution [35–37], in contrast, partial and/or nonclassic intercalation of a ligand may cause a bend or twist in the DNA helix, leading to a decrease of its

effective length [25, 28, 29]. Therefore, viscosity measurements were performed to further clarify the intercalation mode with CT-DNA. When the amounts of all four complexes were increased, the viscosity of CT-DNA increased steadily (Fig. S3), and this is similar to the behavior of ethidium bromide, a well-known DNA intercalator [29, 30, 34–36]. Here, the viscosity measurements suggest that these complexes may bind to CT-DNA through intercalation, in agreement with the UV–vis and fluorescence spectroscopy studies. The experimental viscosity results thus provide strong evidence for the interaction of complexes **1–4** with DNA by intercalation modes and the electronic effect of 1,10-phenanthroline or 2,2'-bipyridine may be an important factor in determining the intrinsic binding constant K_b [33, 38, 44–46].

Thermal denaturation studies provide an additional way to detect intercalation modes [31, 37–39]. The melting temperature (T_m) is the temperature at which the double-stranded DNA dissociates into single strands, and is determined by the hyperchromic effect on the absorption of DNA base pairs ($\lambda = 260 \text{ nm}$). T_m of CT-DNA in the absence of the complexes is $60.7 \pm 0.2 \text{ }^\circ\text{C}$. The observed T_m values in the presence of complexes **1–4** were 65.5 ± 0.2 , 64.2 ± 0.1 , 62.6 ± 0.1 , and $62.0 \pm 0.1 \text{ }^\circ\text{C}$, and ΔT_m was 4.8, 3.5, 1.9, and 1.3 $^\circ\text{C}$, respectively. The T_m values of these complexes are obviously increased compared with T_m of CT-DNA in the absence of the complexes (Fig. S4). Furthermore, complex **1** has a larger DNA-binding affinity than complexes **2–4**.

Cytotoxicity assays

The antitumor activity of all the complexes and ligands against three human-derived cell lines (SH-SY5Y, MCF-7, and SK-N-SH) was evaluated by MTT assays. The IC_{50} values were calculated after 48 h incubation with isoniazid ligands, the four complexes, and cisplatin in different concentrations, respectively. As shown in Table 1, these oxovanadium complexes exhibit broad inhibition of the three human cancer cell lines tested, with IC_{50} values ranging from 1.21 ± 0.13 to $42.2 \pm 4.14 \text{ } \mu\text{M}$, and the antitumor activities are concentration-dependent. Complex **1** possessed the most potent inhibitory effect on the two cell lines. This is consistent with its ability to bind with CT-DNA, indicating that the antitumor properties of the oxovanadium complexes may be closely related to their DNA-binding mode. Previously, we reported that the antiproliferative activity of other oxovanadium(IV) complexes was most likely associated with their DNA-binding abilities [29]. The present results confirmed our previous observations that the antitumor activity of oxovanadium(IV) complexes is associated with their binding abilities and mode of intercalation with DNA.

Table 1 Antiproliferative effects of complexes **1–4** (see Scheme 1 for the structures), cisplatin, and ligands on different cells lines after 48 h treatment

Compounds	IC ₅₀ (μM)		
	SH-SY5Y	MCF-7	SK-N-SH
Cisplatin	7.72 ± 1.34	13.3 ± 1.32	2.95 ± 0.14
PAHN	75.2 ± 1.24	54.0 ± 1.12	47.3 ± 1.19
PAH	82.3 ± 1.28	32.4 ± 1.04	79.5 ± 1.27
VO(acac) ₂	43.61 ± 1.54	>100	20.78 ± 1.54
1	3.95 ± 0.14	1.97 ± 0.21	1.21 ± 0.13
2	6.90 ± 0.38	11.5 ± 0.94	4.10 ± 0.18
3	8.86 ± 0.31	26.5 ± 0.62	2.40 ± 0.34
4	42.2 ± 1.04	17.4 ± 0.45	24.1 ± 0.25

Data are expressed as the 50 % inhibitory concentration (IC₅₀). Cells were treated with various concentrations of the test compounds for 48 h. Cell viability was determined by 3-(4,5-dimethylthiazol-2-yl)-2,5-diphenyltetrazolium bromide assay and IC₅₀ values were calculated as described in “Materials and methods.” Each value represents the mean ± the standard deviation of three independent experiments. PAHN 4-pyridinecarboxylic acid, 2-[(2-hydroxy)-1-naphthalenylene]hydrazide, PAH 4-pyridinecarboxylic acid, 2-[(2-hydroxy)-1-phenyl]methylene hydrazide, acac acetylacetonate

Interestingly, the IC₅₀ values of complex **1** were comparably lower than those of cisplatin under the same conditions. From a comparison of the antitumor activities of their ligands and VO(acac)₂, the four complexes appeared to be more cytotoxic to the SH-SY5Y, MCF-7, and SK-N-SH cell lines. Usually, the pharmacological activity of these types of molecules is often enhanced by complexation with metal ions [33, 45–49]. Among the cell lines under evaluation, the SK-N-SH cells proved to be the most sensitive to treatment with the oxovanadium(IV) complexes.

The micrographs of the SH-SY5Y cell line after treatment for 48 h in the absence of the complexes and in the presence of the different complexes show that the proliferation of SH-SY5Y tumor cells was effectively inhibited (Fig. S5).

Cell cycle analysis

To further define the mechanism of the antiproliferative effect of the oxovanadium(IV) complexes on tumor cells, the cell cycle phase distribution was analyzed by flow cytometry with PI staining [48–51]. According to the results in Table 1, SK-N-SH cells exhibited the highest sensitivity to complex **1**. Thus, this cell line was used for further investigation of the underlying mechanisms accounting for the antiproliferative action of complex **1**. SK-N-SH cells were treated with 0.1, 0.2, and 0.4 μM complex **1**, respectively, for 48 h. The results of the cell cycle analysis in this work showed that the G₂/M phase was arrested significantly after SK-N-SH cells had been

exposed to 0.4 μM complex **1** for 48 h (Table S3). Treatment with 0.1 or 0.2 μM complex **1** resulted in modest phase arrest of SK-N-SH cells at the 48-h time point. There was a significantly increased G₀/G₁ phase distribution and a significantly decreased G₂/M phase distribution in a dose-dependent manner, indicating the induction of G₂/M phase arrest by complex **1**. Moreover, the number of apoptotic cells and the amount of cell debris significantly increased after SK-N-SH cells had been exposed to complex **1**. The results of the cell cycle analysis in this work suggested that the oxovanadium complexes induced proliferative suppression of SK-N-SH cells via the induction of apoptosis [47, 49–51].

Induction of apoptosis as evidenced by Hoechst 33342 staining

Apoptosis is an important continuous process of destruction of undesirable cells during the development or homeostasis in multicellular organisms. This process is characterized by distinct morphological changes including membrane blebbing, cell shrinkage, dissipation of the mitochondrial membrane potential, chromatin condensation, and DNA fragmentation [47, 48].

In an attempt to elucidate whether the G₂/M phase arrest in the SK-N-SH cells induced by complex **1** was associated with apoptosis, we identified the occurrence apoptosis by Hoechst 33342 staining [50–52]. Figure 1 shows representative Hoechst 33258 fluorescence photomicrographs of cultured SK-N-SH cells treated with or without the oxovanadium(IV) complexes. In control cultures (Fig. 1a), nuclei of SK-N-SH cells appeared with regular contours and were round and large. By contrast, the condensation of nuclei characteristic of apoptotic cells was evident in SK-N-SH cells treated with 60 or 120 μM complex **1** for 24 h (Fig. 1c, d). Most nuclei of Jurkat cells treated with complex **1** appeared hypercondensed (brightly stained), and the typical apoptotic bodies were observed, which was different from what was observed in the control cells (Fig. 1c, d). The results indicated that the G₂/M phase arrest in the SK-N-SH cells induced by complex **1** was associated with apoptosis and that the activities are concentration-dependent (Fig. 1b). This may imply that these oxovanadium complexes can cause proliferative suppression of cancer cells via the induction of apoptosis [47–50]. To fully understand the mechanism involved in the induction of apoptosis by the oxovanadium complexes, further investigations will be needed to be conducted.

Scavenging of the hydroxyl radical

It is well known that as one of the most reactive products of reactive oxygen species, the hydroxyl radical could cause

Fig. 1 Apoptosis of SK-N-SH cells induced by complex **1** (see Scheme **1** for the structure). SK-N-SH cells were incubated with complex **1** for 24 h and stained by Hoechst 33342. Almost all cells in the control group were normal. However, apoptotic cells appeared after 24 h treatment with complex **1**. The *arrows* indicate apoptotic cells identified by the Hoechst 33342 staining. **a** The blank control group. **b** Cells with 30 μM complex **1**. **c** Cells treated with 60 μM complex **1**. **d** Cells treated with 120 μM complex **1**

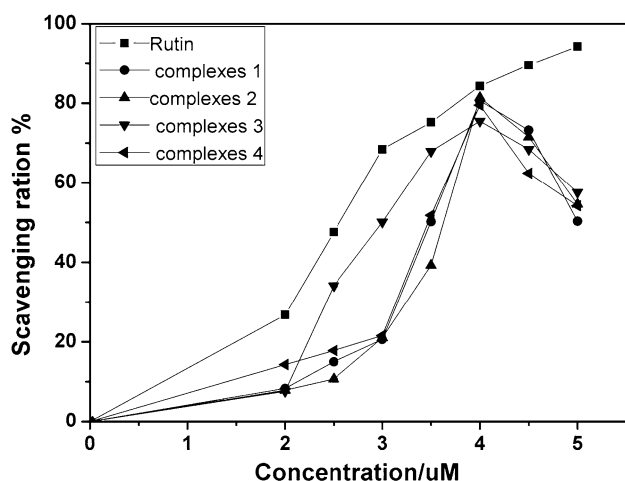
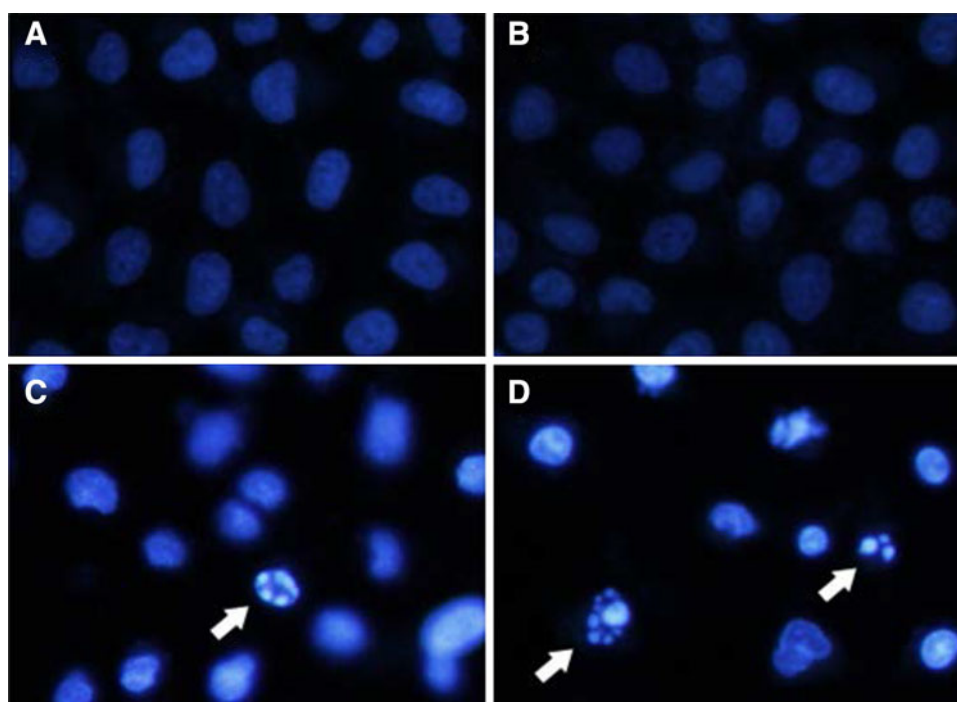


Fig. 2 Scavenging effect of the complexes on hydroxyl radicals (see Scheme **1** for the structures of the complexes **1–4**)

cell membrane disintegration, membrane protein damage, and DNA mutation and further initiate or propagate the development of many diseases [53–55]. Since complexes **1–4** all showed good ability to cleave DNA, it was considered necessary to investigate their scavenging effect on the hydroxy radical. Rutin, which is known to be an effective antioxidant agent [56, 57], was used as a positive control, and the results are shown in Fig. 2.

As shown in Fig. 2, the scavenging effect of complexes **1–4** was concentration-dependent and the scavenging ratio increased on increasing of the concentration of the complexes. The scavenging ratio of the oxovanadium(IV)

complexes reached its peak at 4.0 μM , and then decreased gradually. To the best of our knowledge, there is no information available on the scavenging of the hydroxyl radical by oxovanadium(IV) complexes and/or their scavenging capacity [53–55]. It is well known that antioxidants repress cancer metastasis by *scavenging* reactive oxygen species [53, 56, 57], and so the above results may help understand the mechanism involved in scavenging by oxovanadium complexes in antitumor cells. The mechanism involved in the scavenging of the hydroxyl radical by oxovanadium complexes is under further investigation in our laboratory.

Conclusion

The results reported in this work provide more data related to the interaction of oxovanadium(IV) complexes with DNA. The *in vitro* results provide experimental evidence that oxovanadium(IV) complexes have the potential to be anticancer complexes against human cancer cells. Under certain conditions, these oxovanadium(IV) complexes can scavenge the free radical hydroxyl, a topic that has been only scarcely investigated. Thus, the results obtained from the present oxovanadium(IV) complexes are of importance for the development of metal-based agents for anticancer applications. Further work is in progress to better identify the mechanism of action and to prepare more potent and stabler related oxovanadium compounds for the treatment of cancer.

Acknowledgments We gratefully acknowledge financial support for this work by the Science and Technology Research Project of Guangdong province (no. 2012B031800431), People's Republic of China, and the National Natural Science Foundation of the People's Republic of China (no. 81102753 and no. 21101033).

Conflict of interest The authors declare that there is no conflict of interest.

References

- Gasser G, Ott I, Metzler-Nolte N (2011) *J Med Chem* 54(1):3–25
- Ji LN, Zhou XH, Liu JG (2001) *Coord Chem Rev* 216–217(1): 513–516
- Pasternack RF, Gibbs EJ, Villafranca JJ (1983) *Biochemistry* 22(2):2406–2414
- Bratsos I, Mitri E, Ravalico F, Zangrando E, Gianferrara T, Bergamo A, Alessio E (2012) *Dalton Trans* 41(24):7358–7371
- Hartinger CG, Dyson PJ (2009) *Chem Soc Rev* 38(2):391–401
- Van Rijt SH, Sadler PJ (2009) *Drug Discov Today* 14(23/24):1089–1097
- Gust R, Beck W, Jaouen G, Schoenenberger H (2009) *Coord Chem Rev* 253(21–22):2742–2759
- Schuh E, Pfluger C, Citta A, Folda A, Rigobello MP, Bindoli A, Casini A, Mohr F (2012) *J Med Chem* 55(11):5518–5528
- Wilson JJ, Lippard SJ (2012) *J Med Chem* 55(11):5326–5336
- Angela C (2012) *J Inorg Biochem* 109:97–106
- O'Connor M, Kellett A, McCann M, Rosair G, McNamara M, Orla H (2012) *J Med Chem* 55(5):1957–1968
- Liu WK, Bendorf K, Proetto M, Hagenbach A, Abram U, Gust R (2012) *J Med Chem* 55(8):3713–3724
- Zhang X, Frezza M, Milacic V, Ronconi L, Fan YH, Bi CF, Fregona D, Dou QP (2010) *J Cell Biochem* 109(1):162–172
- Kovala-Demertzi D, Demertzis MA, Miller JR, Papadopoulou C, Dodorou C, Filousis G (2001) *J Inorg Biochem* 86(2–3):555–563
- Thaker BT, Surati KR, Modi CK (2008) *Russ J Coord Chem* 34(3):25–33
- Chohan ZH, Sumrra SH, Youssoufi MH, Hadda TB (2010) *Eur J Med Chem* 45:2739–2747
- Thompson KH, Liboiron BD, Sun Y, Bellman KDD, Setyawati IA, Patrick BO, Karunaratne V, Rawji G, Wheeler J, Sutton K, Bhanot S, Cassidy C, McNeill JH, Yuen VG, Orvig C (2003) *J Biol Inorg Chem* 8:66–74
- Caravan P, Gelmini L, Glover N, Herring FG, Li H, McNeill JH, Rettig SJ, Setyawati IA, Shuter E, Sun Y, Tracey AS, Yuen VG, Orvig C (1995) *J Am Chem Soc* 117:12759–12770
- Tompson KH, McNeill JH, Orvig C (1999) *Chem Rev* 99:2561–2571
- Crans DC, Smee JJ, Gaidamauskas E, Yang L (2004) *Chem Rev* 104:849–902
- Nunes GG, Bonatto AC, de Albuquerque CG, Barison A, Ribeiro RR, Back DF, Andrade AVC, de Sá EL, de Pedrosa FO, Soares JF, de Souza EM (2012) *J Inorg Biochem* 108:36–46
- Tudor R, Maria N, Simona P, Elena P, Donald P, Aurelian G (2010) *Eur J Med Chem* 45:774–781
- Sumrra SH, Chohan ZH (2012) *Spectrochim Acta Part A Mol Biomol Spectrosc* 98:53–61
- Raja DS, Bhuvanesh Nattamai SP, Natarajan K (2012) *Inorg Chim Acta* 385:81–93
- Bishayee A, Waghay A, Patel MA et al (2010) *Cancer Lett* 294(19):1–12
- Benitez J, Becco L, Correia I, Leal SM, Guiset H, Pessoa JC, Lorenzo J, Tanco S, Escobar P, Moreno V, Garat B, Gambino D (2011) *J Inorg Biochem* 105(2):303–312
- Maia Pedro IS, Pavan FR, Leite Clarice QF, Lemos Sebastiao S, de Sousa GF, Batista AA, Nascimento OR, Ellena J, Castellano EE, Niquet E, Deflon VM (2009) *Polyhedron* 28(2):398–406
- Benitez J, Guggeri L, Tomaz I, Arrambide G, Navarro M, Costa Pessoa J, Garat B, Gambino D (2009) *J Inorg Biochem* 103(4):609–616
- Lu JZ, Guo HW, Zeng XD, Zhang YL, Zhao P, Jiang J, Zang LQ (2012) *J Inorg Biochem* 112:39–48
- Lu JZ, Du YF, Guo HW (2011) *J Coord Chem* 64(7):1229–1239
- Du YF, Lu JZ, Guo HW (2010) *Trans Met Chem* 35(7):859–864
- Mannar RM, Manisha B, Nikita C, Amit K, Fernando A, João CP (2012) *Eur J Inorg Chem* 2012:4846–4855
- Nerissa AL, Fange L, Luke S, Anthony M, Travis RE, Jessa FA, Floyd AB, Ramaiyer V (2012) *Eur J Inorg Chem* 2012:664–677
- Puja PH, Anand KP, Shubhra CI, Anjani KT, Sudhir C, Bilikere SD, Anil KM (2012) *Chem Biol Drug Des* 79:223–234
- Barton JK, Raphael AL (1984) *J Am Chem Soc* 106(8): 2466–2468
- Liang XL, Tan LF, Zhu WG (2011) *DNA Cell Biol* 30(1):61–67
- Zhao P, Xu CX, Huang JW, Fu B, Yu HC, Ji LN (2008) *Spectrochim Acta Part A Mol Biomol Spectrosc* 71:1216–1223
- Zhao P, Xu CX, Huang JW, Fu B, Yu HC, Ji LN (2008) *Bioorg Chem* 36:278–287
- Lifeng T, Yue X, Xiaohua L, Sheng Z (2009) *Spectrochim Acta Part A Mol Biomol Spectrosc* 73:858–864
- Natarajan R, Abraham S (2011) *J Mol Struct* 985:173–183
- Babu B, Bhabatosh B, Pijus KS, Basudev M, Ritankar M, Rajan RD, Chakravarty AR (2012) *Eur J Inorg Chem* 2012:126–135
- Kim R (2005) *Cancer* 103(8):1551–1560
- Liu YJ, Zeng CH, Huang HL et al (2010) *J Eur Med Chem* 45(12):564–571
- Li TR, Yang ZY, Wang BD, Qin DD (2008) *Eur J Med Chem* 43(8):1688–1695
- Hwang JH, Larson RK, Abu-Omar MM (2003) *Inorg Chem* 42(24):7967–7977
- Xu HL, Yu XF, Qu SC, Zhang R, Qu XR, Chen YP, Ma XY, Sui DY (2010) *Eur J Pharmacol* 645:14–22
- Vermes I, Haanen C, Steffens-Nakken H, Reutelingsperger C (1995) *J Immunol Methods* 184:39–51
- Thompson CB (1995) *Science* 267:1456–1462
- Martin SJ, Green (1995) *Crit Rev Oncol Hematol* 18:137–153
- Bhabatosh B, Pijus K, Sovan R, Ritankar M, Rajan RD, Akhil RC (2011) *Eur J Inorg Chem* 2011:1425–1435
- Scatena R (2012) *Adv Exp Med Biol* 942:287–308
- Sriram N, Kalayarasan S, Ashokkumar P, Sureshkumar A, Sudhandiran G (2008) *Mol Cell Biochem* 311:157–165
- Syed U, Ganapasam S (2010) *Phytother Res* 24:114–119
- Ashokkumar P, Sudhandiran G (2008) *Biomed Pharmacother* 62:590–597
- Talcott ST, Lee JH (2002) *J Agric Food Chem* 50:3186–3192
- Ray G, Husain SA (2002) *Indian J Exp Biol* 40:1213–1232
- Ozen T, Korkmaz H (2003) *Phytomedicine* 10:405–415